explored, fundamental physical mechanism in the formation of the first stellar objects[2] which may differ from that for stars more metal-rich than [Fe/H] = −4.0.

HE1327–2326 permits exploration of the many formation theories of the earliest stars proposed for HE0107–5240. One idea is the pre-enrichment of the gas clouds from which the two stars formed by a first generation 'faint' type-II supernova ($M \approx 25M_{\odot}$) experiencing mixing and fallback[3], or rotating, massive objects ($M \approx 200$–$300M_{\odot}$; ref. 18). In this case, HE1327–2326 would be an early Population II star, formed from gas enriched by one (or possibly a few) of the first type-II supernovae. In particular, the quantitative predictions of abundance patterns by updated models of 'faint' type-II supernovae (N. Iwamoto, H. Umeda, N. Tominaga and K. Maeda, personal communication) agree with the chemical abundance patterns of HE1327–2326. The diversity of Mg/Fe ratios found in HE1327–2326 and HE0107–5240 is easily explained by the variety of mixing and fallback. A remaining problem is the Sr, whose production is not yet included in these type-II supernova models.

Another idea is the accretion of heavy elements from the interstellar medium onto first-generation low-mass stars (Population III)[1,2,19]. In this case, however, the high abundances of lighter elements must be explained by other processes. The unevolved status of HE1327–2326 means that the scenario in which internal mixing processes lead to the dredge-up of processed material can be excluded. A remaining possibility is mass transfer from an AGB star within a binary system[1,5]. Mass transfer could naturally account for the Li depletion[20] found in HE1327–2326. The high Sr abundance is problematic, along with the non-detection of Ba, which cannot be explained by the s-process expected to occur in AGB stars. A crucial test for this scenario is to check the binarity of this object, for which long-period radial velocity monitoring is required. □

Received 22 November 2004; accepted 8 February 2005; doi:10.1038/nature03455.

1. Christlieb, N. *et al.* A stellar relic from the early Milky Way. *Nature* **419,** 904–906 (2002).
2. Shigeyama, T., Tsujimoto, T. & Yoshii, Y. Excavation of the first stars. *Astrophys. J.* **568,** L57–L60 (2003).
3. Umeda, H. & Nomoto, K. First-generation black-hole-forming supernovae and the metal abundance pattern of a very iron-poor star. *Nature* **422,** 871–873 (2003).
4. Limongi, M., Chieffi, A. & Bonifacio, P. On the origin of HE 0107–5240, the most iron-deficient star presently known. *Astrophys. J.* **594,** L123–L126 (2003).
5. Suda, T., Aikawa, M., Machida, M. N., Fujimoto, M. Y. & Iben, I. Jr. Is HE 0107–5240 a primordial star? The characteristics of extremely metal-poor carbon-rich stars. *Astrophys. J.* **611,** 476–493 (2004).
6. Christlieb, N. *et al.* HE 0107–5240, a chemically ancient star. I. A detailed abundance analysis. *Astrophys. J.* **603,** 708–728 (2004).
7. Wisotzki, L. *et al.* The Hamburg/ESO survey for bright QSOs. III. A large flux-limited sample of QSOs. *Astron. Astrophys.* **358,** 77–87 (2000).
8. Noguchi, K. *et al.* High dispersion spectrograph (HDS) for the Subaru telescope. *Publ. Astron. Soc. Jpn* **54,** 855–864 (2002).
9. Beers, T. C. & Christlieb, N. The discovery and analysis of very metal-poor stars in the galaxy. *Annu. Rev. Astron. Astrophys.* (in the press).
10. Coc, A., Vangioni-Flam, E., Descouvemont, P., Adahchour, A. & Angulo, C. Updated big bang nucleosynthesis compared with Wilkinson microwave anisotropy probe observations and the abundance of light elements. *Astrophys. J.* **600,** 544–552 (2004).
11. Ryan, S. G., Norris, J. E. & Beers, T. C. The Spite lithium plateau: ultrathin but postprimordial. *Astrophys. J.* **523,** 654–677 (1999).
12. Ryan, S. G., Gregory, S. G., Kolb, U., Beers, T. C. & Kajino, T. Rapid rotation of ultra-Li-depleted halo stars and their association with blue stragglers. *Astrophys. J.* **571,** 501–511 (2002).
13. Pinsonneault, M. H., Walker, T. P., Steigman, G. & Narayanan, V. K. Halo star lithium depletion. *Astrophys. J.* **527,** 180–198 (1999).
14. Richard, O., Michaud, G. & Richer, J. Models of metal-poor stars with gravitational settling and radiative accelerations. III. Metallicity dependence. *Astrophys. J.* **580,** 1100–1117 (2002).
15. Aoki, W., Norris, J. E., Ryan, S. G., Beers, T. C. & Ando, H. Detection of lead in the carbon-rich, very metal-poor star LP 625–44: A strong constraint on s-process nucleosynthesis at low metallicity. *Astrophys. J.* **536,** L97–L100 (2000).
16. Travaglio, C. *et al.* Galactic evolution of Sr, Y, and Zr. A multiplicity of nucleosynthetic processes. *Astrophys. J.* **601,** 864–884 (2004).
17. Christlieb, N. *et al.* The Hamburg/ESO R-process enhanced star survey (HERES). I. Project description, and discovery of two stars with strong enhancements of neutron-capture elements. *Astron. Astrophys.* **428,** 1027–1037 (2004).
18. Fryer, C. L., Woosley, S. E. & Heger, A. Pair instability supernovae, gravity waves, and gamma-ray transients. *Astrophys. J.* **550,** 372–382 (2001).
19. Yoshii, Y. Metal enrichment in the atmospheres of extremely metal-deficient dwarf stars by accretion of interstellar matter. *Astron. Astrophys.* **97,** 280–290 (1981).
20. Norris, J. E., Ryan, S. G., Beers, T. C. & Deliyannis, C. P. Extremely metal-poor stars. III. The Li-depleted main-sequence turnoff dwarfs. *Astrophys. J.* **485,** 370–379 (1997).
21. Beers, T. C., Rossi, S., Norris, J. E., Ryan, S. G. & Shefler, T. Estimation of stellar metal abundance. II. A recalibration of the Ca II K technique, and the autocorrelation function method. *Astron. J.* **117,** 981–1009 (1999).
22. Asplund, M. New light on stellar abundances analyses: departures from LTE and homogeneity. *Annu. Rev. Astron. Astrophys.* (in the press).
23. Bessell, M. S., Christlieb, N. & Gustafsson, B. On the oxygen abundance of HE 0107–5240. *Astrophys. J.* **612,** L61–L63 (2004).
24. Alonso, A., Arribas, S. & Martinez-Roger, C. The empirical scale of temperatures of the low main sequence (F0V–K5V). *Astron. Astrophys.* **313,** 873–890 (1996).
25. Yoshii, Y. in *New Trends in Theoretical and Observational Cosmology* (eds Sato, K. & Shiromizu, T.) 235–244 (Universal Academy, Tokyo, 2002).
26. Cutri, R. M., *et al. 2MASS All-Sky Catalog of Point Sources* (California Institute of Technology, Pasadena, 2003); ⟨http://irsa.ipac.caltech.edu/applications/Gator⟩.
27. Girard, T. M. *et al.* The southern proper motion program. III. A near-complete catalog to V = 17.5. *Astron. J.* **127,** 3060–3071 (2004).
28. Kim, Y., Demarque, P., Yi, S. K. & Alexander, D. R. The Y2 isochrones for alpha-element enhanced mixtures. *Astrophys. J. Suppl.* **143,** 499–511 (2002).
29. Kurucz, R. L. *ATLAS9 Stellar Atmosphere Programs and 2 km/s Grid* CD-ROM 13 (Smithsonian Astrophysical Observatory, Cambridge, 1993); ⟨http://kurucz.harvard.edu/cdroms.html⟩.
30. Asplund, M., Grevesse, N. & Sauval, A. J. in *Cosmic Abundances As Records Of Stellar Evolution And Nucleosynthesis* (eds Bash, F. N. & Barnes, T. G.) *ASP Conf. Ser.* (in the press); preprint at ⟨http://www.arxiv.org/astro-ph/0410214⟩ (2004).

Acknowledgements We thank A. Steinhauer and C. Thom for obtaining additional observations, N. Iwamoto, K. Maeda, T. Suda, N. Tominaga and H. Umeda for valuable discussions and L. Wisotzki and D. Reimers for leading the HES. This work was supported by the Astronomical Society of Australia (A.F.), Australian Research Council (M.A., A.F., J.E.N.), Ministry of Education, Culture, Sports, Science and Technology in Japan and JSPS (all Japanese co-authors), Deutsche Forschungsgemeinschaft (N.C.), Swedish Research Council (P.S.B., K.E.), US National Science Foundation (T.C.B.) and JINA (T.C.B., N.C., A.F., J.E.N.). This work is based on data collected at the Subaru Telescope, which is operated by the National Astronomical Observatory of Japan.

Competing interests statement The authors declare that they have no competing financial interests.

Correspondence and requests for materials should be addressed to A.F. (anna@mso.anu.edu.au).

Planet–planet scattering in the upsilon Andromedae system

Eric B. Ford[1], Verene Lystad[2] & Frederic A. Rasio[2]

[1]*Department of Astronomy, University of California, Berkeley, California 94720, USA*
[2]*Department of Physics and Astronomy, Northwestern University, Evanston 60208, Illinois USA*

Doppler spectroscopy has detected 152 planets around nearby stars[1]. A major puzzle is why many of their orbits are highly eccentric; all planets in our Solar System are on nearly circular orbits, as is expected if they formed by accretion processes in a protostellar disk. Several mechanisms have been proposed to generate large eccentricities after planet formation, but so far there has been little observational evidence to support any particular model. Here we report that the current orbital configuration of the three giant planets around upsilon Andromedae[2,3] (υ And) probably results from a close dynamical interaction with another planet[4], now lost from the system. The planets started on nearly circular orbits, but chaotic evolution caused the outer planet (υ And d) to be perturbed suddenly into a higher-eccentricity orbit. The coupled evolution of the system then causes slow periodic variations in the eccentricity of the middle planet (υ And c). Indeed, we show that υ And c periodically returns to a very nearly circular state every 6,700 years.

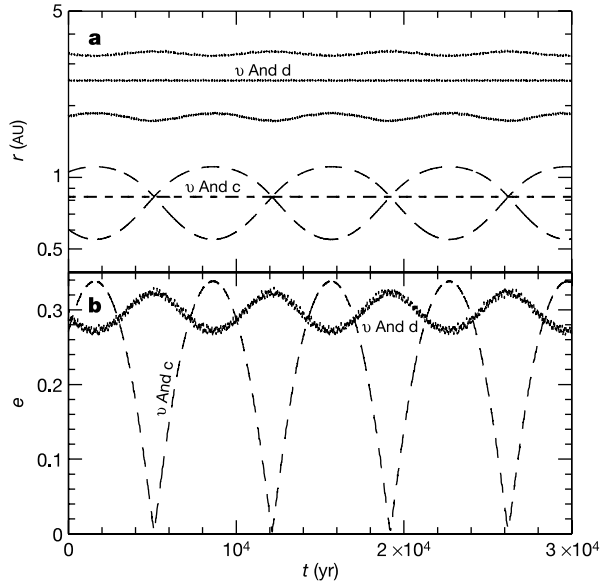

Figure 1 Secular evolution of the planetary system around υ And. **a**, The semimajor axes (middle lines), as well as the periastron and apastron distances (lower and upper lines), for the outer two planets. **b**, The evolution of the orbital eccentricity for each planet. Note that both υ And c (dashed) and υ And d (dotted) have a significant eccentricity at the present time ($t = 0$), but that the eccentricity of υ And c returns periodically to very small values near zero. The results shown here were obtained by direct numerical integration using our best-fit parameters. All direct *N*-body integrations presented in this paper were performed using Mercury, version 6.1 (ref. 21).

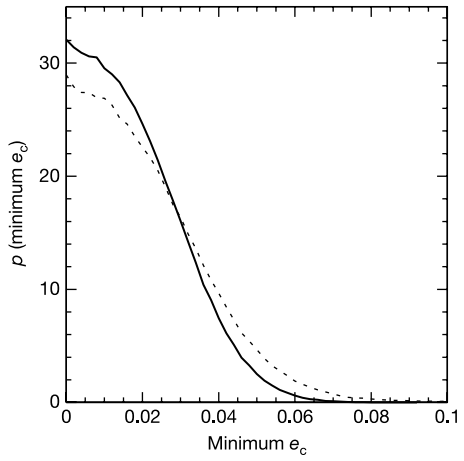

Figure 2 Probability distribution for the minimum eccentricity of υ And c. We draw initial orbital elements for υ And b, c and d from their posterior probability distribution and evolve each system according to classical second-order secular perturbation theory. We find that all allowed orbital solutions have the eccentricity of υ And c oscillating from a maximum value slightly larger than the present value to very nearly zero. The solid curve corresponds to coplanar orbits viewed edge-on. The dotted curve shows the result for orbits with random orientations to the line of sight, but requiring dynamical stability. This implies relative inclinations $<40°$. Note that systems with relative inclinations $>140°$ are also dynamically stable. Although such retrograde orbits are unlikely on theoretical grounds, our conclusions permit this possibility. Because the secular perturbation theory averages over the orbits, it is also valid for retrograde orbits. The fact that all allowed solutions result in the eccentricity of υ And c returning to a very small value can be understood easily from lowest-order secular perturbation theory[4,22], where the eccentricity vector of each planet can be described as the sum of three rotating eigenvectors in the $(e\cos\omega, e\sin\omega)$ plane. The eigenvector representing the effects of υ And b on υ And c has a very small amplitude and can be neglected. For the particular configuration of υ And, the two dominant eigenvectors describing υ And c have very nearly the same length. Depending on whether the eigenvector with the faster rotation (higher eigenfrequency) has a slightly larger or smaller length than the other, the vector sum will be rotating around 360° (circulation) or oscillating with an amplitude close to 90° (libration), respectively. Whenever the two vectors are anti-aligned, the magnitude of their sum, that is, the eccentricity of the planet, is very close to zero; when they are aligned, the eccentricity is maximum.

The innermost planet around υ And has a very small orbital eccentricity, as is expected from tidal circularization[5], but the two outer planets have large eccentricities, both around 0.3. It was quickly recognized after their discovery that the gravitational interaction between these two planets causes significant eccentricity evolution on secular timescales ($\sim 10^4$ years). In particular, in some early solutions, the middle planet's eccentricity appeared to vary periodically with a large amplitude, from a maximum near the present value to a minimum near zero[6]. Later fits to the data suggested that the outer two orbits had arguments of pericentre nearly equal to within about 10°. This could indicate an 'apsidal resonance', in which two elliptical orbits oscillate about an aligned configuration with a small libration amplitude[7].

Two possible explanations have been proposed for this peculiar orbital configuration. The first is a dynamical mechanism in which a sudden perturbation imparts a finite eccentricity to the outer planet[4]. The subsequent secular evolution causes the middle planet's orbit to become eccentric and can leave the two orbits either circulating, or librating with a large amplitude. In either case, the eccentricity of the middle planet periodically returns to its initial low value. The impulsive perturbation of the outer planet would result naturally from planet–planet scattering, which was one of the earliest mechanisms proposed for inducing large eccentricities in extrasolar planets[8,9]. In contrast, the second explanation invokes an adiabatic perturbation of the outer planet's eccentricity through torques exerted by an exterior gaseous disk[10]. As the eccentricity of the middle planet grows on a similarly long timescale, this would leave the system in an apsidal resonance by damping the libration amplitude to zero. This is a natural extension of more general 'migration scenarios' in which the coupling of a planet's orbit to a gaseous disk could both increase eccentricities[11] and lead to orbital decay and the formation of planets with very short orbital periods[12].

Table 1 **Masses and orbital parameters for the three planets in υ And**

Planet	*P* (d)	*e*	ω (deg)	$m\sin i$ (M_J)
b	4.617146(56)	0.016(11)		0.6777(79)
c	241.32(18)	0.258(15)	250.2(4.0)	1.943(35)
d	1301.0(7.0)	0.279(22)	287.9(4.8)	3.943(57)

Results of our new analysis of the υ And radial velocity data[2,3,20]. We have used the entire Lick Observatory data set, kindly provided to us by D. Fischer. For conciseness, we present only the means and standard deviations on the last two digits (indicated in parentheses) after marginalizing over all other parameters. We list the orbital period (*P*) in days, the orbital eccentricity (*e*), the argument of pericentre (ω) in degrees, and the planet mass times the sine of the inclination of the orbital plane to the line of sight ($m\sin i$) in units of Jupiter masses (M_J). More details on our analysis are presented in the Supplementary Information.

The υ And system was the first extrasolar multi-planet system ever discovered by Doppler spectroscopy. Since the first announcement of the outer two planets in 1999, the California and Carnegie Planet Search team has taken over 350 new radial velocity measurements, making υ And one of the systems with the tightest constraints on orbital parameters (Table 1; see also Supplementary Information). The secular evolution of the system is shown in Fig. 1. While the eccentricity of υ And d remains always around 0.3, υ And c returns periodically to a nearly circular orbit with $e < 0.01$. As shown in Fig. 2, this is now a property of all solutions consistent with the data,

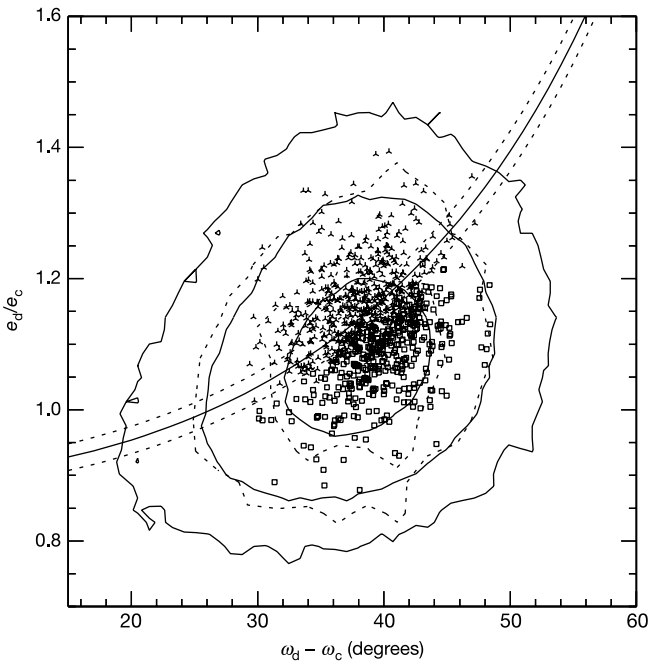

Figure 3 Observational constraints on the secular evolution parameters. The eccentricity ratio is plotted as a function of the difference between the arguments of pericentre for υ And c and d, all at the present epoch. We show the 1-, 2- and 3-σ contours for the posterior probability distribution function marginalized over the remaining fit parameters. The solid contours assume that the radial velocity variations are the result of three non-interacting keplerian orbits viewed edge-on, while the dotted contours include the mutual gravitational interactions of the planets when fitting to the radial velocity data (only 1- and 2-σ contours are shown). The solid line across shows the separatrix between the librating (upper left) and circulating (lower right) solutions according to the classical second-order perturbation theory (neglecting the inner planet, υ And b). The dotted lines on either side show the variation in the location of the separatrix due to the uncertainty in the remaining orbital elements. The data points show the results of our direct numerical integrations for the full three-planet system: tri-stars (squares) indicate that the system was found to be librating (circulating). Note that, regardless of the assumptions, the separatrix runs right through the 1-σ contours. We find the median libration amplitude of the librating systems to be about 80°.

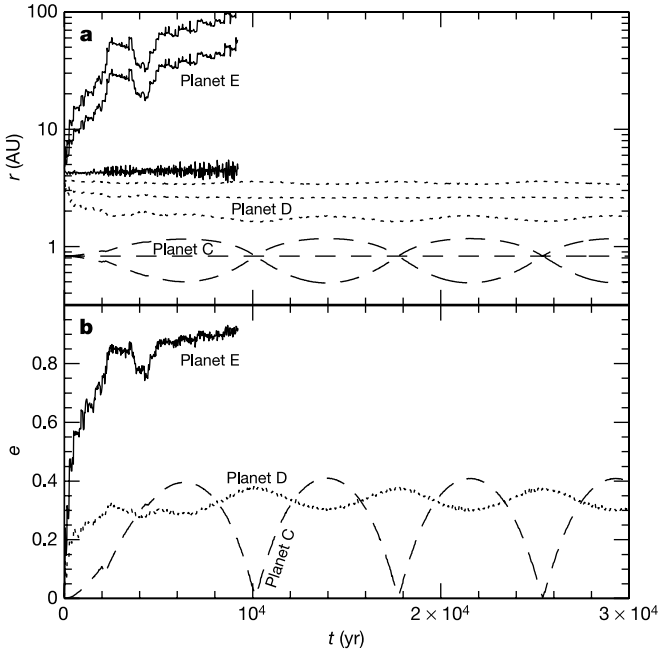

Figure 4 Dynamical evolution of a hypothetical planetary system similar to υ And. Conventions in panels **a** and **b** are as in Fig. 1. Planets B–E are analogous to υ And b, c, d and a hypothetical additional planet. After a brief period of dynamical instability, one planet is ejected, leaving the other two in a configuration very similar to that of υ And c and d. (The innermost planet, B, was not included because it plays a negligible role.) All planets were initially on nearly circular orbits. The initial periods of the two inner planets (C and D) were 241.5 days (equal to the period of υ And c) and 2,100 days. An additional planet (E, solid line), of mass 1.9 M_J, was placed on an orbit of period 3,333 days, so that the outer two planets were close to their dynamical stability limit[23]. The fourth planet (E, solid line) interacted strongly with the third (D, dotted line), while the second planet (C, dashed line) maintained a small eccentricity. After the ejection, the two remaining planets evolve secularly just like υ And c and d (compare with Fig. 1). Although this simulation illustrates a case in which υ And had only one extra planet, our results do not preclude the existence of even more planets at larger distances. In fact, the presence of another planet in an even-longer-period orbit could be responsible for triggering the instability after a long period of seemingly 'stable' evolution and help raise more quickly the pericentre of the planet that perturbed υ And d. Note that the timescale to completely eject the outer planet from the system (after ~9,000 years in this particular simulation) is much longer than the timescale of the initial strong scattering. After this initial brief phase of strong interaction, the perturbations on the outer planet are too weak to affect significantly the coupled secular evolution of υ And c and d. Thus, the 'initial' eccentricity of υ And c for the secular evolution is determined by its value at the end of the strong interaction phase, rather than that at the time of the final ejection.

in contrast to earlier suggestions that it could happen for some solutions[4,6].

We have also re-examined the possible presence of apsidal resonance in the system. Remarkably, we find that the allowed solutions all lie very close to the boundary between librating and circulating configurations (Fig. 3). As a consequence, all librating systems have libration amplitudes close to 90°. As shown in Fig. 3, this behaviour is confirmed by direct numerical integrations of all three planets for a large sample of systems covering the allowed parameter space of solutions.

Our results do not change significantly if the assumption of a coplanar system viewed edge-on is relaxed. Inclination angles can be constrained by requiring dynamical stability of the system[6,7,13,14]. Using the most recent data we find that, for a coplanar configuration of three planets with the best-fit orbital parameters, the system becomes dynamically unstable when $\sin i < 0.5$ (where $\sin i = 1$ corresponds to edge-on). If we relax coplanarity, we find that the system becomes dynamically unstable whenever the relative inclination is greater than about 40°. Throughout the full range of allowed inclination angles we find qualitatively similar behaviour for the secular evolution of the system. For example, Fig. 2 shows that the eccentricity of υ And c would still return periodically to a value near zero. The secular evolution of the system should be re-evaluated if future observations of υ And were to discover an additional planet (which would be termed υ And e) in a long-period orbit.

Our analysis clearly confirms that the υ And system is evolving exactly as would be expected after an impulsive perturbation to υ And d (ref. 4). The initial sudden change in eccentricity for the outer planet would be naturally produced by a close encounter with another planet, which was ejected from the system as a result. Using our knowledge of planet–planet scattering from several previous studies[8,15–17], we determined plausible initial conditions for the original, unstable system. The early dynamical evolution of such a system is illustrated in Fig. 4. After a brief period of strongly chaotic evolution, lasting ~10^3 years, the outer planet is ejected, and the remaining two planets are left in a dynamical configuration closely resembling that of υ And (see Supplementary Information for a more detailed discussion).

While several other mechanisms (for example, perturbations in a binary star[18], resonances[10], interaction with a gaseous disk[11]) have been proposed to explain the large eccentricities of extrasolar planets, only planet–planet scattering naturally results in an impulsive perturbation—which is necessary to explain the υ And system. All other mechanisms operate on much longer timescales and would also affect the eccentricity of υ And c, erasing the memory of its initial circular orbit (see Supplementary Information for a more detailed discussion).

Our results have other implications for planet formation. Given the difficulty of forming giant planets at small orbital distances, it is generally assumed that the υ And planets migrated inward to their current locations via interactions with the protoplanetary disk[12]. If this is correct, then the small minimum eccentricity of υ And c also provides evidence that its eccentricity at the end of migration had not grown significantly, in contrast to what some theories predict[11]. However, the possibility of formation *in situ*[19] cannot be excluded by our results. □

Received 18 October 2004; accepted 3 February 2005; doi:10.1038/nature03427.

1. Schneider, J. *Extra-solar Planets Catalog* ⟨http://cfa-www.harvard.edu/planets/catalog.html⟩ (2005).
2. Butler, R. P. *et al.* Evidence for multiple companions to Upsilon Andromedae. *Astrophys. J.* **526,** 916–927 (1999).
3. Fischer, D. A. *et al.* A planetary companion to HD 40979 and additional planets orbiting HD 12661 and HD 38529. *Astrophys. J.* **586,** 1394–1408 (2003).
4. Malhotra, R. A dynamical mechanism for establishing apsidal resonance. *Astrophys. J. Lett.* **575,** L33–L36 (2002).
5. Rasio, F. A., Tout, C. A., Lubow, S. H. & Livio, M. Tidal decay of close planetary orbits. *Astrophys. J.* **470,** 1187–1191 (1996).
6. Stepinski, T. F., Malhotra, R. & Black, D. C. The Upsilon Andromedae system: models and stability. *Astrophys. J.* **545,** 1044–1057 (2000).
7. Chiang, E. I., Tabachnik, S. & Tremaine, S. Apsidal alignment in Upsilon Andromedae. *Astron. J.* **122,** 1607–1615 (2001).
8. Rasio, F. A. & Ford, E. B. Dynamical instabilities and the formation of extrasolar planetary systems. *Science* **274,** 954–956 (1996).
9. Weidenschilling, S. J. & Marzari, F. Gravitational scattering as a possible origin for giant planets at small stellar distances. *Nature* **384,** 619–621 (1996).
10. Chiang, E. I. & Murray, N. Eccentricity excitation and apsidal resonance capture in the planetary system Upsilon Andromedae. *Astrophys. J.* **576,** 473–477 (2002).
11. Goldreich, P. & Sari, R. Eccentricity evolution for planets in gaseous disks. *Astrophys. J.* **585,** 1024–1037 (2003).
12. Lin, D. N. C. *et al.* in *Protostars and Planets IV* (eds Mannings, V., Boss, A. P. & Russell, S. S.) 1111–1178 (Univ. Arizona Press, Tucson, 2000).
13. Lissauer, J. J. & Rivera, E. J. Stability analysis of the planetary system orbiting Upsilon Andromedae. II. Simulations using new Lick Observatory fits. *Astrophys. J.* **554,** 1141–1150 (2001).
14. Lystad, V. & Rasio, F. in *The Search for Other Worlds* (eds Holt, S. S. & Deming, D.) 273–276 (AIP Conf. Proc. 713, American Institute of Physics, New York, 2004).
15. Ford, E. B., Havlickova, M. & Rasio, F. A. Dynamical instabilities in extrasolar planetary systems containing two giant planets. *Icarus* **150,** 303–313 (2001).
16. Ford, E. B., Rasio, F. A. & Yu, K. in *Scientific Frontiers in Research on Extrasolar Planets* (eds Deming, D. & Seager, S.) 181–187 (ASP Conf. Ser. 294, Astronomical Society of the Pacific, San Francisco, 2003).
17. Marzari, E. F. & Weidenschilling, S. J. Eccentric extrasolar planets: the jumping Jupiter model. *Icarus* **156,** 570–579 (2002).
18. Holman, M., Touma, T. & Tremaine, S. Chaotic variations in the eccentricity of the planet orbiting 16 Cyg B. *Nature* **386,** 254–256 (1997).
19. Bodenheimer, P., Hubickyj, O. & Lissauer, J. J. Models of the in situ formation of detected extrasolar giant planets. *Icarus* **143,** 2–14 (2000).
20. Ford, E. B. Quantifying the uncertainty in the orbits of extrasolar planets. *Astron. J.* (in the press).
21. Chambers, J. E. A hybrid symplectic integrator that permits close encounters between massive bodies. *Mon. Not. R. Astron. Soc.* **304,** 793–799 (1999).
22. Murray, C. D. & Dermott, S. F. *Solar System Dynamics* (Cambridge Univ. Press, New York, 1999).
23. Gladman, B. Dynamics of systems of two close planets. *Icarus* **106,** 247–265 (1993).

Supplementary Information accompanies the paper on **www.nature.com/nature**.

Acknowledgements We are very grateful to D. Fischer for providing us with the latest radial velocity data on υ And. We also thank E. Chiang, M. H. Lee and S. Peale for discussions. This work was supported by an NSF grant to F.A.R. at Northwestern University and by a Miller Research Fellowship to E.B.F. V.L. acknowledges support from the NASA Undergraduate Summer Research Program at Northwestern. F.A.R. and E.B.F. thank the Kavli Institute for Theoretical Physics for hospitality and support.

Competing interests statement The authors declare that they have no competing financial interests.

Correspondence and requests for materials should be addressed to F.A.R. (rasio@northwestern.edu).

Sensitivity gains in chemosensing by lasing action in organic polymers

Aimée Rose[1], Zhengguo Zhu[1], Conor F. Madigan[2], Timothy M. Swager[1] & Vladimir Bulović[2]

[1]*Department of Chemistry and* [2]*Department of Electrical Engineering and Computer Science, Massachusetts Institute of Technology, Cambridge, Massachusetts 02139, USA*

Societal needs for greater security require dramatic improvements in the sensitivity of chemical and biological sensors. To meet this challenge, increasing emphasis in analytical science has been directed towards materials and devices having highly nonlinear characteristics; semiconducting organic polymers (SOPs), with their facile excited state (exciton) transport, are prime examples of amplifying materials[1–3]. SOPs have also been recognized as promising lasing materials[4], although the susceptibility of these materials to optical damage has thus far limited applications. Here we report that attenuated lasing in optically pumped SOP thin films displays a sensitivity to vapours of explosives more than 30 times higher than is observed from spontaneous emission. Critical to this achievement was the development of a transducing polymer with high thin-film quantum yield, a high optical damage threshold in ambient atmosphere and a record low lasing threshold. Trace vapours of the explosives 2,4,6-trinitrotoluene (TNT) and 2,4-dinitrotoluene (DNT) introduce non-radiative deactivation pathways[5] that compete with stimulated emission. We demonstrate that the induced cessation of the lasing action, and associated sensitivity enhancement, is most pronounced when films are pumped at intensities near their lasing threshold. The combined gains from amplifying materials and lasing promise to deliver sensors that can detect explosives with unparalleled sensitivity.

One of the successes for SOP-based sensors has been the ultra-trace detection of vapours of TNT and DNT using SOP thin films[5], which enables the detection of buried landmines on the basis of an explosive vapour signature[6]. The detection of TNT/DNT is facilitated by the electron-deficient-acidic nature of nitroaromatics that bind to the electron-rich semiconducting polymer and quench its fluorescence by an electron transfer mechanism. The emission quenching is enhanced when the excitons rapidly diffuse throughout the SOPs, thereby increasing the probability of an encounter with the TNT/DNT. The low vapour pressure of DNT and TNT (about 100 p.p.b. and 5 p.p.b., respectively) and their efficiency for reversible fluorescence quenching make them ideal analytes to explore novel sensitivity augmentation mechanisms in SOP sensors. Previous approaches to increasing the signal gain in these systems focused on extending the exciton diffusion length by increasing excited state lifetimes and by producing emissive three-dimensional electronic delocalization[7,8]. Here we demonstrate a different enhancement mechanism that can complement all of these other schemes by harnessing the amplifying nature of the SOP lasing action to generate greater sensitivity. We demonstrate with this new approach a more than 30-fold increase in detection sensitivity when operating near the lasing threshold.

Lasing in both SOPs[4] and molecular organic materials[9,10] can generally be obtained for materials with high photoluminescence efficiencies and large Stokes shifts (that minimize the light reabsorption losses)[11]. However, a limitation of these organic materials has been the lack of durability under the punishing conditions of high pump powers, ambient atmosphere and extended operation, all of which are necessary for many sensory applications. Polymer **1** (Fig. 1) was designed to meet these demanding photophysical and stability needs and also to be sensitive to the chosen analytes, TNT